

# Variability Science in Accretion Disk Theory

Ryoji Matsumoto,<sup>1</sup> Mami Machida,<sup>2</sup> and Hiroshi Oda<sup>3</sup>

<sup>1</sup> Department of Physics, Graduate School of Science, Chiba University

<sup>2</sup> National Astronomical Observatory

<sup>3</sup> Graduate School of Science and Technology, Chiba University

*E-mail(RM): matumoto@astro.s.chiba-u.ac.jp*

## ABSTRACT

Global three-dimensional magnetohydrodynamic simulations of black hole accretion disks enable us to study the time variabilities of black hole accretion disks without introducing the phenomenological  $\alpha$  viscosity. Numerical simulations including optically thin radiative cooling revealed that when the disk luminosity exceeds  $0.01L_{\text{Edd}}$ , where  $L_{\text{Edd}}$  is the Eddington luminosity, cooling instability taking place in the low/hard state disk creates a magnetically supported, optically thin luminous disk (high/hard state disk) whose X-ray luminosity exceeds  $0.1L_{\text{Edd}}$  when the accretion rate continues to increase. We found that when the outer region of the disk ( $r > 20r_s$ , where  $r_s$  is the Schwarzschild radius) undergoes this transition, an inner torus is formed in  $r < 10r_s$ . The inner torus produces low-frequency quasi-periodic oscillations (QPOs) and high-frequency QPOs whose frequency are  $1 - 10\text{Hz}$ , and  $\sim 100\text{Hz}$ , respectively for stellar mass black holes, and  $10^{-6} - 10^{-5}\text{Hz}$ , and  $\sim 10^{-4}\text{Hz}$ , respectively for Seyfert galaxies with black hole mass  $10^7 M_\odot$ . When the magnetic energy stored in the disk is released, the disk completes the transition to an optically thick, high/soft state. Monitoring observations by MAXI will detect these transitions in stellar mass black holes and QPOs in AGNs.

KEY WORDS: Accretion: Accretion Disk – Black Hole – Magnetohydrodynamics – QPO

## 1. Introduction

Black hole candidates (BHCs) show time variabilities whose time scale ranges from dynamical time scale to viscous time scale of accretion disks. The rotation period of the disk around a Schwarzschild black hole with mass  $M$  is  $t_{\text{rot}} = 2\pi/(GM/r_{\text{ms}}^3)^{1/2} \sim 5 \times 10^{-4} M/M_\odot \text{sec}$  at the last stable orbit  $r_{\text{ms}} = 3r_s$  where  $r_s$  is the Schwarzschild radius. This period is about 5ms in galactic BHCs ( $M \sim 10M_\odot$ ), 30min for our galactic center black hole ( $M \sim 4 \times 10^6 M_\odot$ ), and about 1 day for a supermassive black hole with mass  $M \sim 2 \times 10^8 M_\odot$ . The rotation period can be shorter for Kerr black holes. When the innermost region of the black hole accretion disk has one-armed structure or a hot spot, the disk luminosity observed from the direction near the equatorial plane will change with this rotation time scale.

Quasi-periodic oscillations (QPOs) sometimes observed in galactic BHCs can also be produced by disk oscillations (e.g., Kato 2001). Typical angular frequency of the radial disk oscillation at radius  $r$  is the epicyclic frequency (frequency of the radial oscillation around a circular Keplerian orbit)  $\kappa(r) = [(GM/r^3)(1 - 3r_s/r)]^{1/2}$  in disks around a Schwarzschild black hole. This frequency has maximum  $\kappa_{\text{max}} = 0.0625(GM/r_s^3)^{1/2} \sim 0.045(r_s/c)$  at  $r = 4r_s$ . The oscillation period  $t_{\text{osc}}$  corresponding to

$\kappa_{\text{max}}$  is  $t_{\text{osc}} \sim 1.4 \times 10^{-3}(M/M_\odot)\text{sec}$ . The period of high frequency QPOs in galactic BHCs is the same order as  $t_{\text{osc}}$ . It indicates that high frequency QPOs are excited in the innermost region of the disk. Since the frequency of high frequency QPOs strongly depends on the metric of space time, it gives us clues to measure the mass and spin of the black hole.

The power spectral density (PSD) of X-ray time variations in galactic BHCs in low/hard state show  $1/f$  spectrum around 1Hz. The slope of the PSD becomes flatter in  $f < 0.1\text{Hz}$  and steeper in  $f > 10\text{Hz}$ . The low frequency time variations in Cyg X-1 are characterized by the X-ray shots which take place with interval of several seconds (Negoro et al. 2001). Machida and Matsumoto (2003) showed by global three-dimensional resistive magnetohydrodynamic (MHD) simulations that X-ray shots are produced by magnetic reconnection in the innermost plunging region of the disk. Smaller scale magnetic reconnections ubiquitously taking place in the disk create  $1/f$  X-ray fluctuations (Kawaguchi et al. 2000).

Galactic BHCs sometimes show outbursts. During an outburst, the BHCs undergo transition from a low/hard state to a high/soft state. This transition typically takes days but Machida et al. (2006) showed by 3D MHD simulations that the transition from a low/hard state to an in-

intermediate high/hard (luminous hard) state takes place in thermal time scale  $t_{\text{th}} \sim t_{\text{dyn}}/\alpha$ , where  $t_{\text{dyn}}$  is the dynamical time scale, and  $\alpha$  is the viscosity parameter introduced in conventional theories of accretion disks. This time scale is less than 1 sec in galactic BHCs and days-month in AGNs. We will discuss the physical mechanism of the hard-to-soft transitions in section 3.

In galactic BHCs, high frequency QPOs are observed when the source luminosity exceeds  $0.1L_{\text{Edd}}$ , where  $L_{\text{Edd}}$  is the Eddington luminosity. In AGNs with  $M \sim 5 \times 10^7 M_{\odot}$ , the period of the high frequency QPOs will be around 1 day. Long time scale observations by MAXI will be able to detect high frequency QPOs in such AGNs. Galactic BHCs also show low frequency QPOs whose frequency is several Hz and increases with the luminosity. In AGNs with  $M \sim 5 \times 10^7 M_{\odot}$ , the period of low frequency QPOs will be 10 days-1 month. We would like to discuss the excitation mechanisms of the low frequency QPOs in section 4 (see also Machida et al. 2008 and Machida's paper in this proceedings).

## 2. Three-dimensional MHD Simulations of Radiatively Inefficient Black Hole Accretion Disks

Angular momentum of the rotating plasma should be transported outward or extracted from the disk to enable the accretion of the disk material. The thermal time scale and viscous time scale of an accretion disk depend on the efficiency of the angular momentum transport. In conventional theory of accretion disks, the angular momentum transport is incorporated by introducing the  $\alpha$  parameter by assuming that the  $r\varphi$ -component of the stress tensor is proportional to pressure,  $t_{r\varphi} = \alpha P$ . By comparing the theory and observation of dwarf novae,  $\alpha$  is estimated to be 0.01-0.1. However, 3D hydrodynamical simulations of black hole accretion disks revealed that the hydrodynamical turbulence excited in the disk is too weak (e.g., Hawley 1991). This puzzle was resolved by taking into account the magnetic fields and magnetic turbulence generated by the magneto-rotational instability (MRI; Balbus and Hawley 1991). Three-dimensional MHD simulations of a local part of the disk showed that magnetic fields are amplified

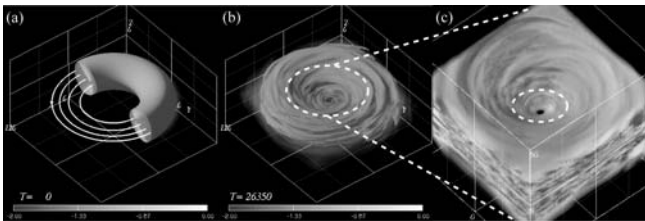


Fig. 1. Results of a 3D MHD simulation of formation of a black hole accretion disk. Grey scale shows density. (left) Initial state. White curves show magnetic field lines. (middle) Quasi-steady state. (right) Enlargement of the innermost region of the accretion disk.

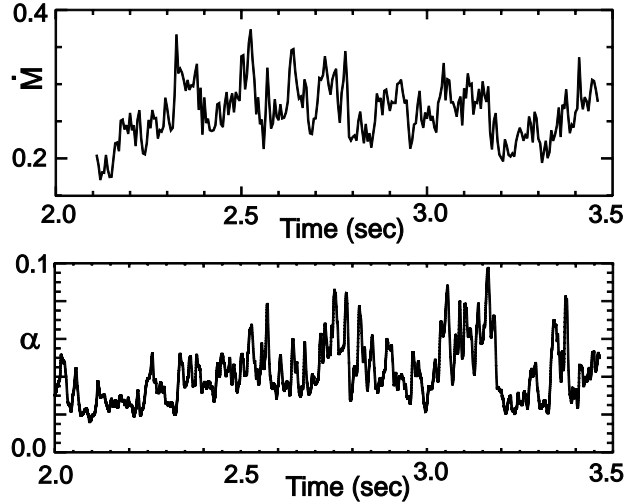


Fig. 2. Time variations of accretion rate measured at  $r = 2.5r_s$  and efficiency of angular momentum transport  $\alpha = \langle -B_r B_\varphi / (4\pi) \rangle / P$  obtained from global 3D MHD simulations of accretion disks (Machida and Matsumoto 2008). The time unit is 1 sec for  $10M_{\odot}$  black hole.

until the magnetic pressure  $p_{\text{mag}}$  becomes about 10% of the gas pressure  $p_{\text{gas}}$  (i.e.,  $\beta = p_{\text{gas}}/p_{\text{mag}} \sim 10$ ), and that the Maxwell stress transports angular momentum with efficiency  $\alpha = \langle -B_r B_\varphi / (4\pi) \rangle / P \sim 0.01 - 0.1$ . These results have been confirmed by global 3D MHD simulations (e.g., Matsumoto 1999; Hawley 2000; Machida et al. 2000).

Figure 1 shows a result of global 3D MHD simulations of a torus initially threaded by weak azimuthal magnetic fields (Machida and Matsumoto 2003). Assuming that the torus is optically thin and radiatively inefficient, we neglected the radiative cooling term in the energy equation. General relativistic effects are simulated by using the pseudo-Newtonian potential  $\phi = -GM/(r - r_s)$ . In figure 1, density distribution is depicted by grey-scale. White curves in the left panel show magnetic field lines. As the MRI grows, the initial torus is deformed into an accretion disk by efficiently transporting the angular momentum. The disk material spirally infalls toward the central black hole.

Figure 2 shows the time variation of the mass accretion rate measured at  $r = 2.5r_s$  (top panel) and the time variation of the efficiency of the angular momentum transport  $\alpha$  in the quasi-steady state. The unit of time is 1 sec for  $10M_{\odot}$  black hole. The time unit can be scaled arbitrary in proportion to the black hole mass. The accretion rate and  $\alpha$  show large amplitude fluctuations similar to the X-ray light curves of black hole candidates. The range of  $\alpha$  ( $= 0.01 - 0.1$ ) is consistent with the values conventionally assumed in disk models based on the  $\alpha$  prescription of viscosity.

Figure 3 shows the PSD of time variabilities of mass

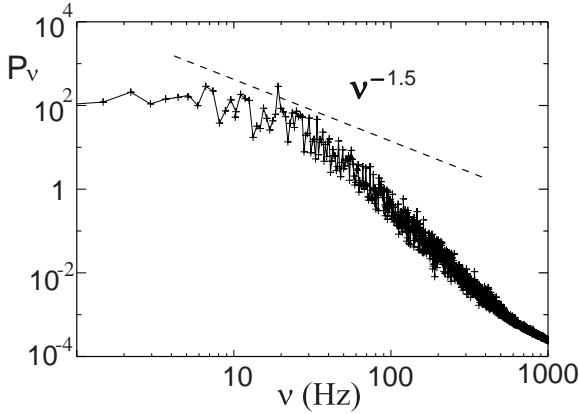


Fig. 3. Power spectral density of time variation of accretion rate obtained from a MHD simulation of radiatively inefficient, hot disk.

accretion rate obtained from global 3D MHD simulations of optically thin, hot disk (Machida and Matsumoto 2008). It reproduces the  $1/f$  fluctuations around 10Hz observed in stellar mass black holes and steepening of the PSD in  $\nu > 10\text{Hz}$ .

### 3. Hard-to-Soft State Transition

During an outburst of galactic black hole candidates, they undergo hard-to-soft state transition. The top panel of figure 4 schematically shows the color-luminosity diagram of the evolution of an outburst. An outburst starts from the X-ray hard, low luminosity state (low/hard state). The X-ray luminosity of the source increases almost preserving the X-ray color (from the right bottom to the right top). When the luminosity attains  $\sim 0.1L_{\text{Edd}}$ , the source undergoes a transition to the high/soft state.

The bottom panel of figure 4 shows the theoretically obtained thermal equilibrium curves of accretion disks (Abramowicz et al. 1995). The left branch is an optically thin branch, and the right branch is an optically thick branch. The upper half of the optically thin branch corresponds to the low/hard state, in which the advective cooling balances with the heating. Such accretion flows are called advection dominated accretion flows (ADAF; e.g., Narayan & Yi 1994) or radiatively inefficient accretion flows (RIAF). Such disks are hot ( $T \sim 10^{11}\text{K}$ ), optically thin, and emit hard X-rays. Since the radiative cooling rate increases with the accretion rate, optically thin thermal equilibrium disappears when the accretion rate exceeds the threshold. The disk will then undergo a transition to the optically thick, high/soft state. The critical luminosity for this transition is  $\sim 0.01L_{\text{Edd}}$  when  $\alpha = 0.01 - 0.1$ . However, BHCs often stay in hard state even when their luminosity exceeds the theoretically expected threshold for the hard-to-soft transition.

Machida et al. (2006) carried out global 3D MHD

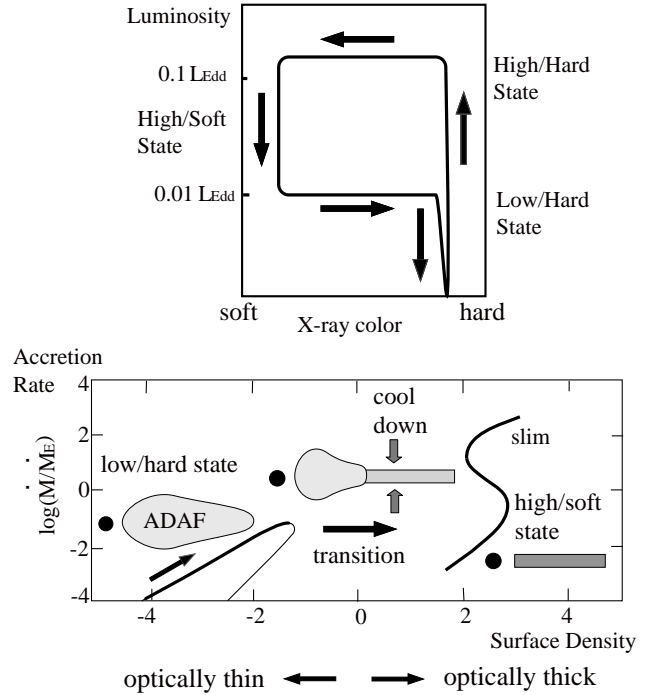


Fig. 4. (top) A schematic color-luminosity diagram of the time evolution of black hole outbursts. (bottom) Thermal equilibrium curves of black hole accretion disks (Abramowicz et al. 1995).

simulations of black hole accretion disks including optically thin radiative cooling. The top panel of figure 5 shows the result of the simulation without including the radiative cooling. Geometrically thick, hot disk is formed. The bottom panel of figure 5 shows the density (left) and temperature (right) of the disk obtained by a simulation including the radiative cooling. As the cooling instability grows, the disk shrinks in the vertical direction and forms a dense, cool disk in the equatorial region. Since the critical accretion rate for the cooling instability is higher in the inner region closer to the black hole, inner regions of the disk ( $r < 10r_s$ ) still stays in the low density, hot state.

We found that since the disk shrinks in the vertical direction almost conserving the mean azimuthal magnetic flux, magnetic field is amplified in the disk and that the disk is supported by magnetic pressure. Figure 6 shows the evolution of the density, temperature, and plasma  $\beta$  in the equatorial region. As the cooling instability grows, magnetic pressure dominant (low  $\beta$ ), cool disk is formed. Once a low- $\beta$  disk is formed, buoyant escape of the magnetic flux will be suppressed because the Parker instability is stabilized by the magnetic tension (Shibata et al. 1990). Since the cooling balances with the heating in such disks, the low- $\beta$  disk stays in a quasi-steady state. Such disks are optically thin because the disk cannot shrink in the vertical direction due to the

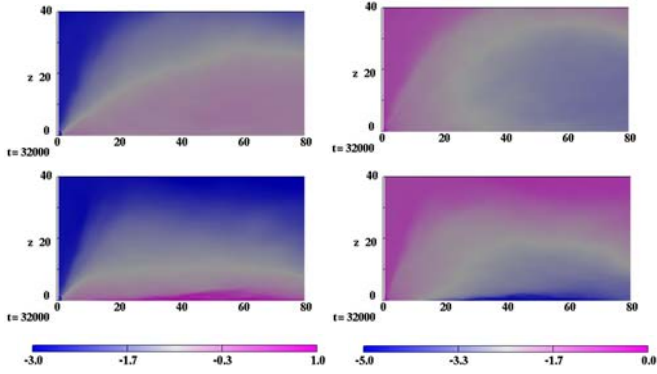


Fig. 5. Results of global 3D MHD simulations of black hole accretion disks. Left panels show the density, and the right panels show the temperature. (top) Without cooling. (bottom) A result of simulation including optically thin radiative cooling. Dense, cool disk is formed in the equatorial region.

enhanced magnetic pressure. The low- $\beta$  disk explains why black hole candidates stay in X-ray hard state even when their luminosity exceeds the threshold for the onset of the cooling instability.

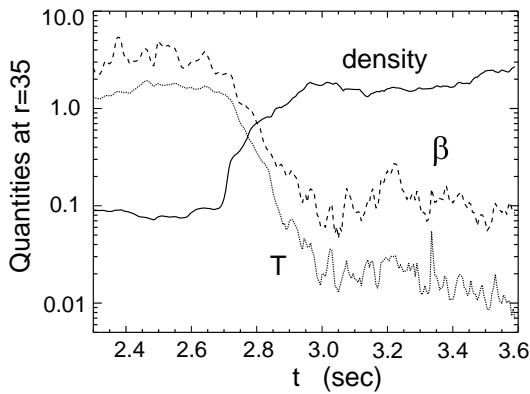


Fig. 6. Time evolution of density, temperature, and plasma  $\beta$  at the equatorial plane during the cooling instability for  $10M_{\odot}$  black hole.

We obtained thermal equilibrium curves of black hole accretion disks taking into account the mean azimuthal magnetic fields (Oda et al. 2007, 2008). Figure 7 shows a result using the cooling function applicable both to optically thin and thick region. The parameter  $\zeta$  denotes the radial advection rate of azimuthal magnetic flux. We assumed that the  $r\varphi$ -component of stress tensor is proportional to the total pressure including the gas pressure, magnetic pressure, and the radiation pressure. We found that when the azimuthal magnetic flux is large enough ( $\zeta > -1$ ), low- $\beta$  branch connects the optically thin branch and the optically thick branch. During the hard-to-soft transition, the black hole candidate will evolve quasi-steadily along this equilibrium curve until their X-ray luminosity approaches  $L_{\text{Edd}}$ . We can explain the existence of the high/hard (or bright

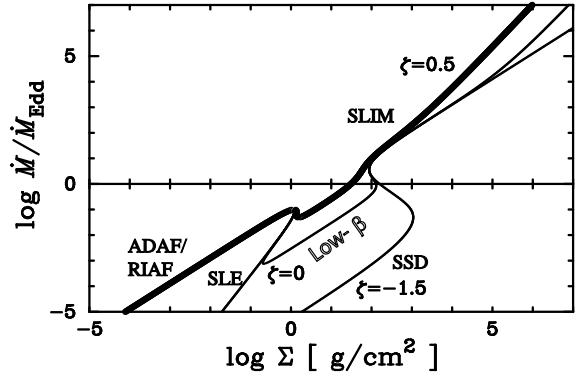


Fig. 7. Thermal equilibrium curves of black hole accretion disks including azimuthal magnetic field (Oda et al. 2008). Magnetic pressure supported equilibrium state (low- $\beta$  branch) connects the optically thin ADAF/RIAF branch and the optically thick SSD (Shakura Sunyaev Disk) and SLIM disk branch.

hard) state by this low- $\beta$  branch. When the mass accretion rate is close to the Eddington mass accretion rate  $\dot{M}_{\text{Edd}} = L_{\text{Edd}}/(\eta c^2)$ , where  $\eta$  is the energy conversion efficiency which we take  $\eta = 0.1$ , limit-cycle oscillation is expected between the low- $\beta$  branch and the slim disk branch. A galactic microquasar GRS1915+105 may stay in this state.

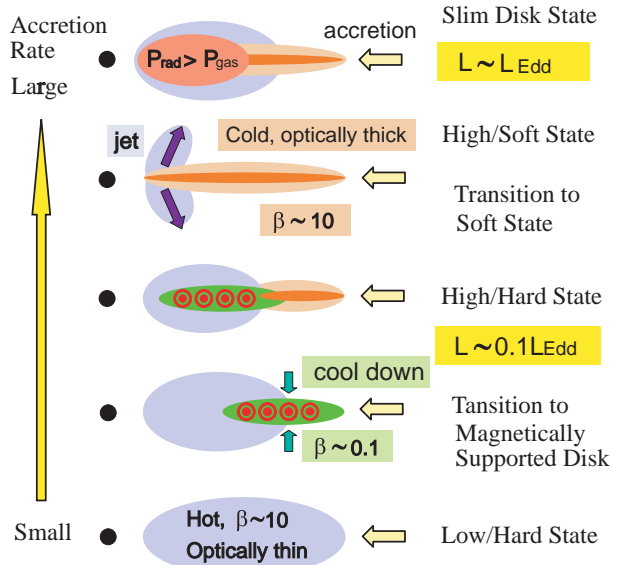


Fig. 8. A schematic picture of the evolution of magnetized black hole accretion disks.

Figure 8 schematically shows the evolution of a black hole candidate during an outburst. When the accretion rate increases and the X-ray luminosity exceeds  $0.01L_{\text{Edd}}$ , cooling instability takes place in the outer region of the disk. When  $L \sim 0.1L_{\text{Edd}}$ , the cooling instability takes place in the innermost region close to the black hole. When the magnetic energy stored in the low-

$\beta$  disk is released by magnetic reconnection or buoyant rise of the magnetic flux, relativistic jets will be launched from the innermost region of the disk. When the accretion rate increases further, radiation pressure supported slim disk will be formed. Narrow line Seyfert galaxies whose luminosity is close to  $L_{\text{Edd}}$  may stay in this state.

#### 4. Quasi Periodic Oscillations of Black Hole Accretion Disks

In galactic black hole candidates, quasi periodic oscillations are observed when their luminosity is high ( $L > 0.1L_{\text{Edd}}$ ). It indicates that QPOs appear when the cooling instability takes place in the disk. We carried out global 3D MHD simulations starting from a cool, outer torus at  $r = 50r_s$  (Matsumoto et al. 2007, Machida et al. 2008). We found that when cool gas accretes to the black hole, an inner torus is formed in  $r < 10r_s$  because angular momentum transport rate decreases. When the magnetic field is weak, the inner torus subjects to the non-axisymmetric instability known as the Papaloizou Pringle instability (Papaloizou & Pringle 1984) and deforms itself into a crescent shape (figure 9). Magnetic fields are strongly amplified in the deformed torus. Figure 10 shows the time variation of the magnetic energy and Joule heating rate. Quasi-periodic sawtooth like oscillation is excited. This oscillation is driven by the magnetic field amplification and subsequent release of magnetic energy due to magnetic reconnection. As the magnetic energy is amplified and  $\beta$  approaches unity, magnetic reconnection taking place in the disk releases the magnetic energy stored in the disk and restores the disk into a weakly magnetized state. Subsequently, non-axisymmetric instability grows and magnetic energy is amplified again. The period of the sawtooth-like oscillation is about 10 rotation period of the inner torus, which corresponds to 1-10Hz in stellar mass black holes. This

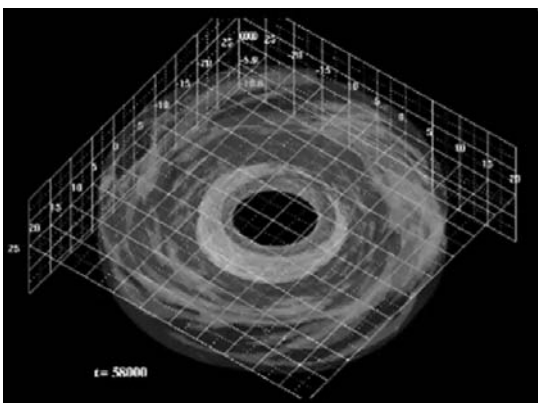


Fig. 9. Formation of an inner torus and growth of non-axisymmetric structure in the inner torus. Grey scale shows density.

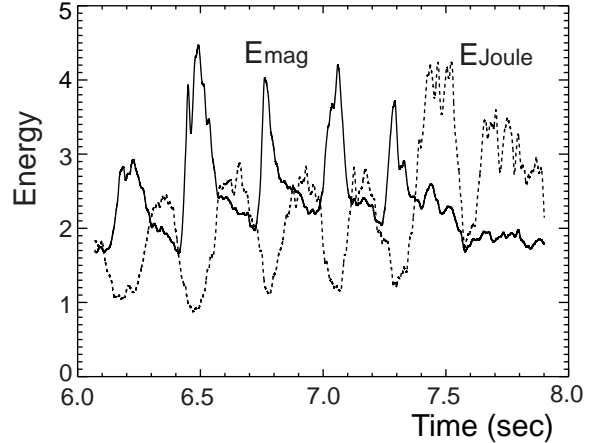


Fig. 10. Sawtooth-like oscillation in the inner torus around a  $10M_{\odot}$  black hole obtained from global 3D MHD simulation of cool accretion flows (Matsumoto et al. 2007).

frequency coincides with the low frequency QPOs (LFQPOs) observed in galactic black hole candidates.

Figure 11 shows the power spectral density of the time variation of mass accretion rate when the sawtooth-like oscillation is excited in the inner torus. Twin peak high frequency oscillations (HFQPOs) with frequency ratio 2:3 are also excited (Matsumoto et al. 2007).

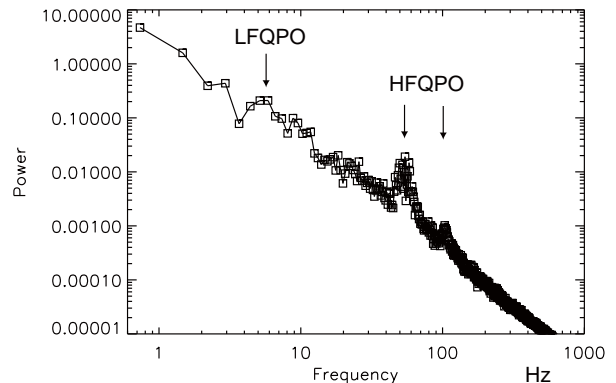


Fig. 11. Power spectral density of time variation of accretion rate at  $r = 2.5r_s$  obtained from the global 3D MHD simulation of a cool accretion flow around a  $10M_{\odot}$  black hole.

#### 5. Summary and Discussion

Global 3D MHD simulations of black hole accretion disks reproduced  $1/f$  fluctuations of low/hard state disks, and low frequency QPOs and high frequency QPOs observed in luminous disks. Global simulations including radiative cooling showed that a magnetically supported (low- $\beta$ ) disk is formed during the hard-to-soft transition. The low- $\beta$  disk is geometrically slim, optically thin and spectrally hard until their luminosity approaches the Eddington luminosity. These results explain why black hole

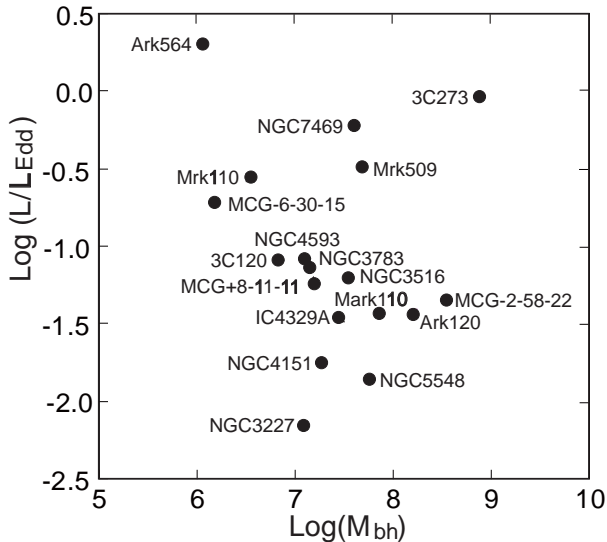


Fig. 12. Black hole mass and the ratio of their luminosity to the Eddington luminosity for nearby Seyfert galaxies and quasars whose X-ray flux exceeds 10mCrab.

candidates stay in high/hard state even when their luminosity exceeds the upper limit for the existence of radiatively inefficient, optically thin disk (ADAF/RIAF)

The transition from ADAF/RIAF to low- $\beta$  disk proceeds from the outer region of the disk. When the outer disk is cooled by this transition, the cool accreting gas forms an inner torus in  $r < 10r_s$ . We showed that low frequency QPOs are excited in the inner torus and that the inner torus is deformed into a crescent shape. When the disk is observed from the direction close to the equatorial plane, periodic time variabilities with time scale of the rotation period of the inner torus will be observed. Numerical simulations also indicate that the low frequency QPOs accompany high frequency QPOs.

The period of the low frequency QPOs is about 10 rotation period of the inner torus ( $0.01 - 0.1M/M_\odot$  sec). The period will be  $10^5 - 10^6$  sec in Seyfert galaxies whose black hole mass is  $10^7M_\odot$ . Figure 12 plots the black hole mass and X-ray luminosity normalized by the Eddington luminosity for nearby Seyfert galaxies and quasars whose X-ray luminosity exceeds 10mCrab. We adopted the black hole mass and X-ray luminosity reported by Turner et al. (1999) and Bian & Zhao (2003). More than 10 galaxies exist in the luminosity range we expect low frequency QPOs ( $0.01L_{\text{Edd}} - 1L_{\text{Edd}}$ ). MAXI will be able to detect low frequency QPOs from these AGNs. Higher time-resolution observations by Suzaku or XMM will be able to detect high frequency QPOs.

Another interesting time variability of BHCs is the relaxation oscillation between the gas pressure (or magnetic pressure) dominant disk and radiation pressure dominant slim disk (Honma et al. 1991). The quasi periodic bursts observed in GRS1915+105 can be ex-

plained by this mechanism. The period of the relaxation oscillation is  $\sim 10M/M_\odot$  sec. We expect similar relaxation oscillations with period  $\sim 10^7$ sec in narrow line Seyfert galaxies such as Ark564 whose X-ray luminosity is  $\sim L_{\text{Edd}}$  and black hole mass  $M \sim 10^6M_\odot$ .

We thank T. Kawaguchi for summarizing the black hole mass and X-ray luminosity of nearby AGNs shown in figure 12. Numerical simulations were carried out by using VPP5000 at National Astronomical Observatory, Japan. This work is supported by the Grants-in-Aid for Scientific Research of Ministry of Education, Culture, Sports, Science, and Technology (RM: 17030003, 20340040).

## References

- Abramowicz, M.A. et al. 1995, ApJ, 438, L37  
Balbus, S.A., & Hawley, J.F. 1991, ApJ, 376, 214  
Bian W., & Zhao, Y. 2000, ApJ, 591, 733  
Hawley, J.F. 1991, ApJ, 381, 496  
Hawley, J.F. 2000, ApJ, 528, 462  
Honma, F., Matsumoto, R., & Kato, S. 1991, PASJ, 43, 147  
Kato, S. 2001, PASJ, 53, 1  
Kawaguchi et al. 2000, PASJ, 52, L1  
Machida, M., Hayashi, M.R., & Matsumoto, R. 2000, ApJ, 532, L67  
Machida, M., & Matsumoto, R. 2003, ApJ, 585, 429  
Machida, M., Nakamura, K.E., & Matsumoto, R. 2006, PASJ, 58, 193  
Machida, M., & Matsumoto, R. 2008, PASJ, 60, 613  
Matsumoto, R. 1999, Proceedings of the International Conference on Numerical Astrophysics 1998, Ed. S. Miyama et al., Kluwer Academic (Astrophysics and Space Science Library v240), p.195  
Matsumoto, R., & Machida, M. 2007, Proceedings of IAU Symposium 238, Black Holes from Stars to Galaxies - Across the Range of Masses, Ed. V. Karas, G. Matt, Cambridge University Press, p.37  
Narayan, R., & Yi, I. 1994, ApJ, 428, L13  
Negoro, H., Kitamoto, H., & Mineshige, S. 2001, ApJ, 554, 528  
Oda, H., Machida, M., Nakamura, K.E., & Matsumoto, R. 2007, PASJ, 59, 457  
Oda, H., Machida, M., Nakamura, K.E., & Matsumoto, R. 2008, Astrophysics of Compact Objects, AIP Conference Proceedings, 968, p.408  
Papaloizou, J.C.B., & Pringle, J.E. 1984, MNRAS, 208, 721  
Shibata, K., Tajima, T., & Matsumoto, R. 1990, ApJ, 350, 295  
Turner, T.J., George, I.M., Nandra, K., & Turcan, D. 1999, ApJ, 524, 667